POLITECNICO DI TORINO
Repository ISTITUZIONALE

NO2 Concentrations and COVID-19 in Local Systems of Northwest Italy (Chapter 7)

Original
NO2 Concentrations and COVID-19 in Local Systems of Northwest Italy (Chapter 7) / Sarzotti, E., Pignocchino, G., Pezzoli, A., Besana, A. - In: Post Un-Lock / Brunetta Grazia, Lombardi Patrizia, Voghera Angioletta. - ELETTRONICO. - Cham : Springer, 2023. - ISBN 978-3-031-33893-9. - pp. 83-98 [10.1007/978-3-031-33894-6_7]

Availability:
This version is available at: 11583/2980079 since: 2023-07-08T10:46:07Z

Publisher:
Springer

Published
DOI:10.1007/978-3-031-33894-6_7

Terms of use:

This article is made available under terms and conditions as specified in the corresponding bibliographic description in the repository

Publisher copyright

(Article begins on next page)

25 November 2026

Chapter 7
NO_2 Concentrations and COVID-19 in Local Systems of Northwest Italy



Ettore Sarzotti, Gianmarco Pignocchino, Alessandro Pezzoli, and Angelo Besana

Abstract This paper aims to further investigate the relationship between the concentrations of nitrogen dioxide (NO_2) and the severity of COVID-19 by analyzing the data of three Italian Regions (Piedmont, Valle d'Aosta and Liguria) during the first wave of the pandemic (February–May 2020). The analyses were conducted at a local scale using Local Labor Systems of ISTAT. The annual average of NO_2 concentrations, obtained from space satellite Sentinel-5P, was used to assess environmental data. While excess mortality data were used to estimate the severity of the pandemic, calculated as the percentage change in deaths recorded in 2020 compared to the average number of deaths of the previous five years (2015–2019). Using quasi-Poisson multivariate regression models, it was possible to estimate the correlation between the incidence rate of the pandemic and some risk factors, including in particular the concentration of NO_2.

Keywords COVID-19 · Nitrogen dioxide · Local systems

7.1 Introduction

The northern regions have been the most affected area by the first wave of the COVID-19 epidemic in Italy. The great speed and intensity with which disease has spread to these regions has led to the hypothesis, in some preliminary studies, that high levels of pollution may play a role in epidemic expansion and in determining the severity of the infection (Coccia 2020; Conticini et al. 2020; Fattorini and Regoli 2020; Martelletti

E. Sarzotti (✉) · G. Pignocchino
Università degli Studi di Torino, Turin, Italy
e-mail: ettore.sarzotti@gmail.com

A. Pezzoli
DIST—Interuniversity Department of Regional and Urban Studies and Planning, Politecnico di Torino, Turin, Italy

A. Besana
Humanities Department, University of Trento, Trento, Italy

© The Author(s) 2023

G. Brunetta et al. (eds.), *Post Un-Lock*, The Urban Book Series,
https://doi.org/10.1007/978-3-031-33894-6_7

and Martelletti 2020). In fact, Northern Italy is one of the most heavily polluted area in Europe in terms of smog and air pollution (Carugno et al. 2016) because it is characterized by a high concentration of densely populated urban areas, as well as by a strong presence of industrial activities. In addition, the particular geomorphological conformation and the weather-climatic characteristics of some areas do not favor the recirculation and release of pollutants with their consequent stagnation.

This contribution intends to verify these hypotheses at a more detailed geographical scale than the previous studies (Fattorini and Regoli 2020; Pignocchino et al. 2022), that is to say at the level of local systems, considering the northwestern regions of Italy, that are characterized by different environmental conditions and socio-demographic patterns. The results should therefore have a greater geographical consistency and, therefore, scientific validity.

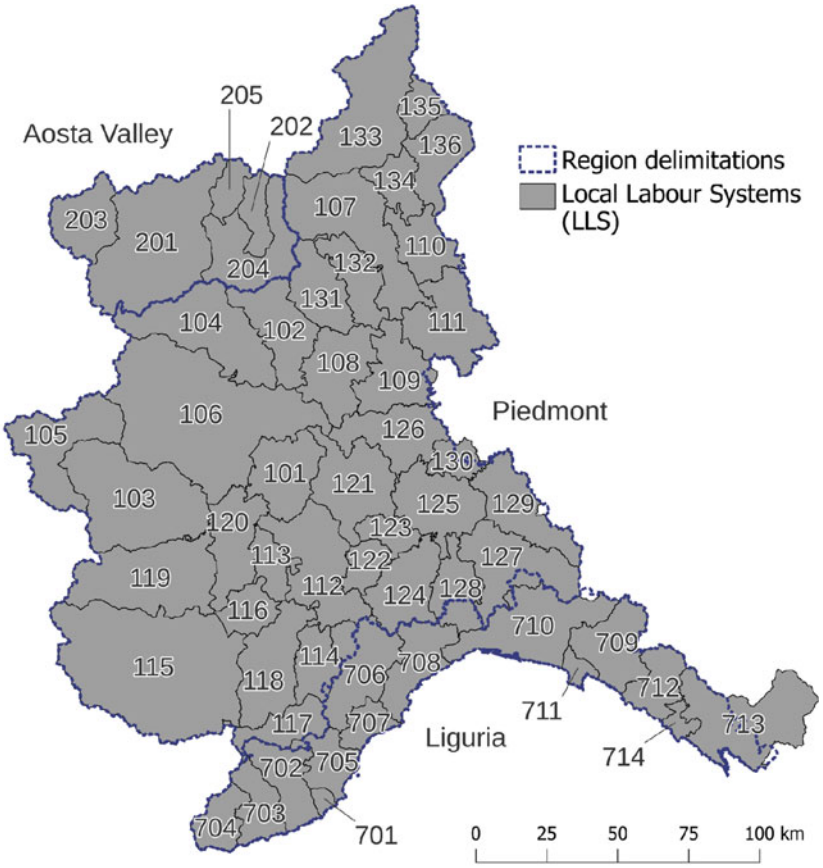
7.2 Materials and Methods

This research project focused on the period of the first COVID-19 epidemic wave (February–May 2020) in the Northwest regions. We worked on the data at the local level by considering Local Labor Systems (LLS), which are inter-municipal territorial units, independent from any administrative subdivision, and defined by the daily commuting flows recorded in the general population and housing censuses (ISTAT 2015a).

In order to analyze this data at the local level, the first necessary step was to create a cartography of LLS updated to the most recent changes in the administrative boundaries of the municipalities using the data referring to January 1, 2020, obtained by ISTAT—Italian National Institute of Statistics (ISTAT 2020a). The total number of LLS in Piedmont, Valle d'Aosta and Liguria regions is 55 (Fig. 7.1).

From the first months of the pandemic, a discrepancy is emerged between official data on COVID-19 deaths and the significantly higher number of deaths compared to previous years (Ciminelli and Garcia-Mandicó 2020). Therefore, to estimate the real impact of COVID-19, we used excess mortality data, defined as the percentage of change in the mortality of the year 2020 compared to the average number of deaths in the same period of the previous five years (2015–2019). These data were retrieved from ISTAT (ISTAT 2021a), temporally aggregated bi-weekly and then for the overall period (February-May).

Nitrogen dioxide (NO_2) concentrations data were derived from the space satellite Sentinel 5 Precursor (S5P) managed by the European Space Agency (ESA) under the Copernicus program. According to Eum et al. (2019), there is an association between one year of exposure to nitrogen dioxide and the increase of mortality from several pathologies (cardiovascular and respiratory, in particular). Therefore, we decided to consider the time period of one year as proxy for the pollution data. The data were retrieved from the Sentinel-5P OFFL NO_2 dataset through Google Earth Engine platform (GEE), obtaining a single grid image defined by the annual mean of NO_2 concentrations from July 1, 2018 to June 30, 2019 with a resolution of 1 km^2 per



LLS Code	LLS Denomination	LLS Code	LLS Denomination	LLS Code	LLS Denomination
101	CHIERI	120	SAVIGLIANO	201	AOSTA
102	IVREA	121	ASTI	202	AYAS
103	PINEROLO	122	CANELLI	203	COURMAYEUR
104	RIVAROLO CANAVESE	123	NIZZA MONFERRATO	204	SAINT-VINCENT
105	SUSA	124	ACQUI TERME	205	VALTOURNENCHE
106	TORINO	125	ALESSANDRIA	701	DIANO MARINA
107	BORGOSESIA	126	CASALE MONFERRATO	702	IMPERIA
108	SANTHIÀ	127	NOVI LIGURE	703	SANREMO
109	VERCELLI	128	OVADA	704	VENTIMIGLIA
110	BORGOMANERO	129	TORTONA	705	ALBENGA
111	NOVARA	130	VALENZA	706	CAIRO MONTENOTTE
112	ALBA	131	BIELLA	707	FINALE LIGURE
113	BRA	132	COSSATO	708	SAVONA
114	CEVA	133	DOMODOSSOLA	709	CHIAVARI
115	CUNEO	134	OMEGNA	710	GENOVA
116	FOSSANO	135	SANTA MARIA MAGGIORE	711	RAPALLO
117	GARESSIO	136	VERBANIA	712	SESTRI LEVANTE
118	MONDOVÌ			713	LA SPEZIA
119	SALUZZO			714	LEVANTO

Fig. 7.1 LLS of Piedmont, Valle d'Aosta, and Liguria

pixel.[1] Pollution data of nitrogen dioxide for the first period of the epidemic wave (February to May) were also collected in the form of nine grids, each with the average concentration referenced over a two-week interval.

Next to this, population-weighted average was calculated using a grid image from the Gridded Population of the World dataset of the Center for International Earth Science Information Network (CIESIN 2018). This grid was also used to derive the population density (population/km^2) of each local system.

The Italian National Institute of Statistic was the source of the data on the resident population as of January 1, 2020 (ISTAT 2020b) and for LLS quality indicators (ISTAT 2015b). Among many quality indicators, three were used in this study: the number of jobs, from which it was derived the number of jobs per capita (jobs/population), and two self-containment indices (SCI), one referred to the jobs demand and the other to the jobs supply. The self-containment index of the demand (SCID) is calculated as the number of workers who work and live in the LLS divided by the number of workers who are working there, while the self-containment index of the supply (SCIS) is calculated as the rate between the number of workers who work and live in the LLS and the number of workers who are living there. These indices vary from 0 to 1 and quantify the level of isolation of the local systems, i.e., higher values of SCID index correspond to fewer workers who come from outside the LLS to work, while higher values of SCIS index correspond to fewer residents who work outside the LLS.

All data not available at the local system level were obtained at the municipality level and then aggregated to LLS.

An exploratory and descriptive analysis was conducted for each variable considered in this study, using histograms and boxplots to investigate the distributions of the values and detect the presence of outliers, and finally cartograms to evaluate the spatial distribution. To assess the effect of emergency measure taken by the Italian government (lockdown) on air pollution, a series of maps of the bi-weekly period of NO_2 concentrations was created. In addition, for each bi-weekly period, a cartogram on excess mortality data was also created to visualize the spatial and temporal evolution of the pandemic.

Spearman's correlation coefficient[2] was used to examine the relationship between nitrogen dioxide concentrations and excess mortality. Next to this, three quasi-Poisson regression models were implemented to exploring further the relationship between the two variables. Poisson's multivariate regression models are generalized linear models based on a logarithmic scale. They are useful with counting variables (number of deaths, in this case) and for modeling rates. A generalization of Poisson models was used in this study: the quasi-Poisson regression, which allows to take

[1] The tropospheric vertical column of NO_2 was considered and the concentrations values were transformed from mol/m^2 to μmol/m^2 for an easier consultation.

[2] A nonparametric index based on the ordinal position of the values (ranks), which fits better with variables that present outliers since is less affected from them. This coefficient varies from -1 to $+1$, where values close to zero indicates no correlation and values close to 1 means a strong correlation (negative or positive).

in account the overdispersion of the data by adjusting the variance to a specific dispersion parameter (Berk and MacDonald 2008).

Within these models, other variables were considered for a possible confounding effect on the associations between the two main variables: the population density, the proportion of the population over the age of 65 (population over 65/total population), the proportion of the male population (male population/total population), the number of jobs per capita, the LLS self-containment index of the demand, and the LLS self-containment index of the supply. These confounding factors were chosen as the data show higher mortality among males and among the elderly people. More deaths are expected in areas with higher population density while higher number of jobs and the level of isolation measured by the self-containment indices could represent a limitation to the spread of the virus within local systems.

Results obtained from the quasi-Poisson multivariate regression models are expressed as estimated rate ratio (RR), a relative difference used to compare different observed incidence rates due to exposure to a given risk factor over a given time period. In this study, the rate ratio is calculated as the ratio of the incidence rate in an exposed group and the incidence rate in a less exposed group. The risk factor is the NO_2 concentrations.

All cartograms were created with QGIS platform and all statistical analysis were carried out with RStudio software.

7.3 Results

7.3.1 Descriptive Analysis

All the variables used in this study have a tendency toward a normal distribution, as shown in the histograms in Fig. 7.2 The most extreme values, numerically distant from the rest of the data collected, are identifiable as outliers and only the two self-containment indices are the variables that do not present with one, as also confirmed by the boxplots in Fig. 7.3.

The effects of the limitations to circulation, imposed by the Italian government with a national lockdown, in LSS considered are visible in Fig. 7.4. The reduction in NO_2 concentrations starts from the 9th week, and there is a constant decreasing trend of the values recorded for the whole lockdown period (weeks 11–18). The end of the national restrictions marks the return to higher values as shown in weeks 19–20.

A good visualization of the first evolution wave is represented in Fig. 7.5. The cartograms show the excess mortality in the nine bi-weekly periods considered from weeks 5 and 6 (January 27–February 9) to weeks 21 and 22 (May 18–31) in all LLS used in this study. It is evident that the excess mortality started in weeks 9–10 when the number of local systems with excess mortality was greater than 50% (Fig. 7.6). The peak was reached in weeks 13–14, with only one local system without excess mortality, and began to fade after weeks 15–16. It is noticeable that the most affected

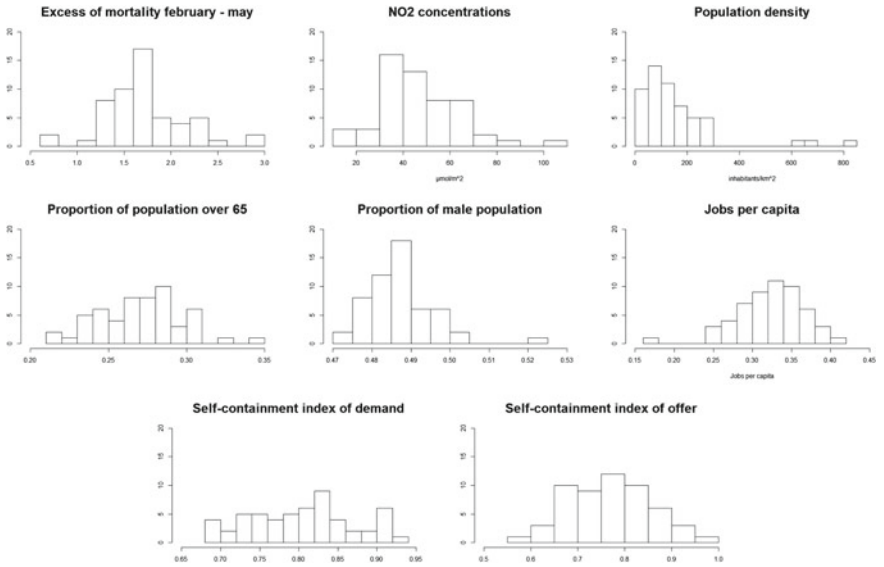


Fig. 7.2 Histograms of variables

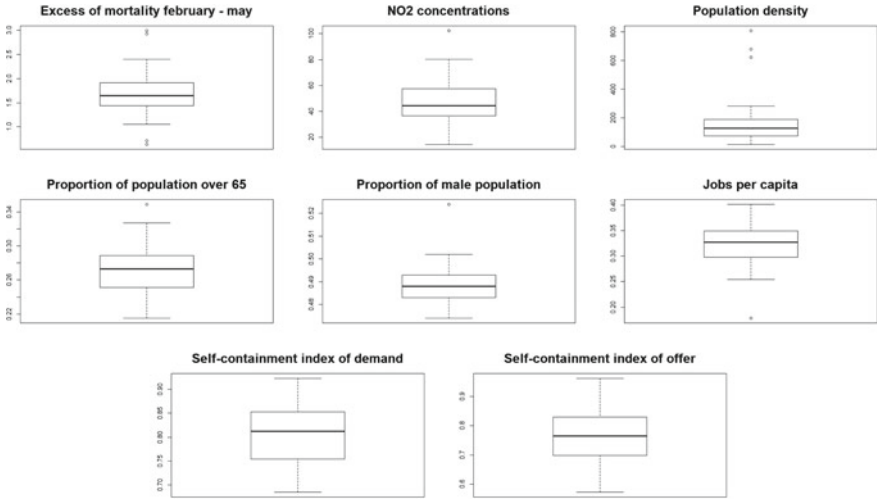


Fig. 7.3 Boxplots of variables

period, which runs from weeks 11 to 18, corresponded to the national lockdown that started on March 9 (DPCM 2020a) and ended on May 4 (DPCM 2020b).

Considering the excess mortality for the whole period of the first wave (Fig. 7.7a), a pattern of higher values emerges close to the border with Lombardy region, although not well defined since some border LLS report only medium values. Other clusters

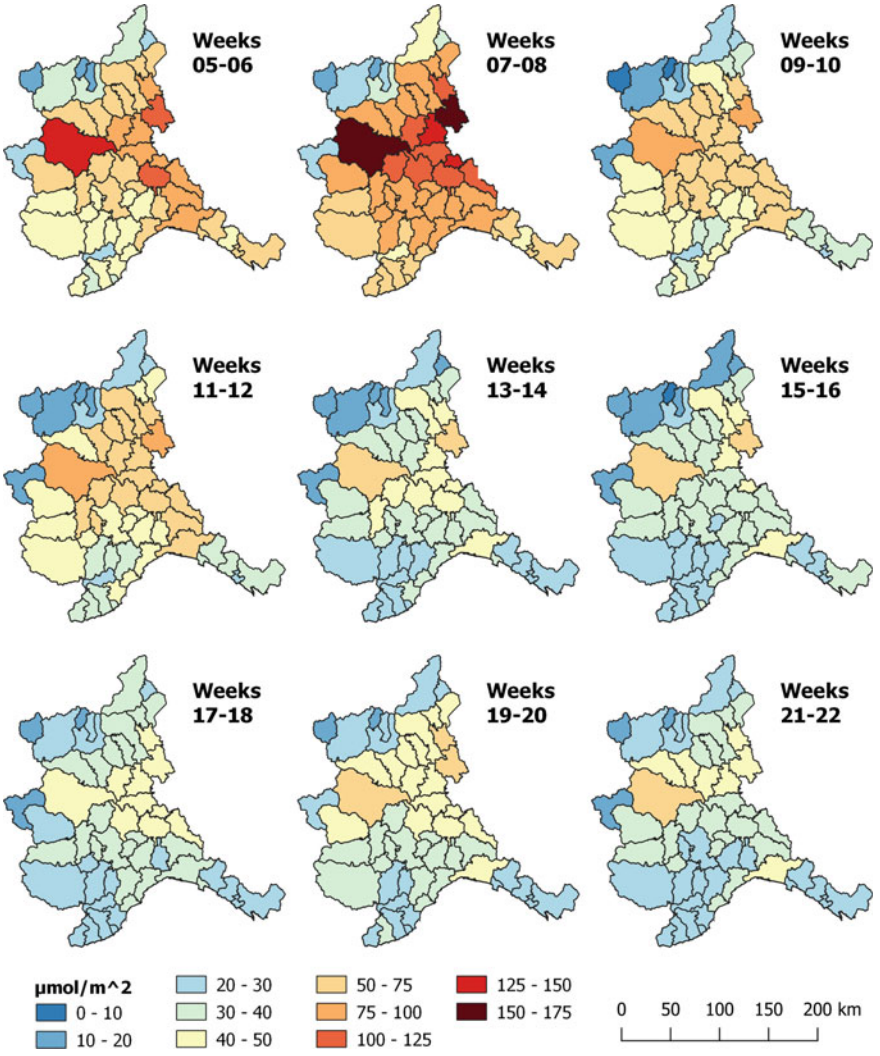


Fig. 7.4 Average concentrations of NO_2 for LLS

of high values far from it are the local system of Garessio and the axis Tortona–Turin. This pattern becomes more evident in the cartogram of NO_2 concentrations (Fig. 7.7b) where a group of local system with medium–high values on the eastern border is clearly visible. The values tend to decrease toward West except for Turin LLS which corresponds to the outlier value.

Not all variables present a clear pattern like the previous; however in the cartogram of the population density (Fig. 7.8a), it is possible to see a spatial correlation with the NO_2 concentrations, which is confirmed by a Pearson correlation index of 0.51 with

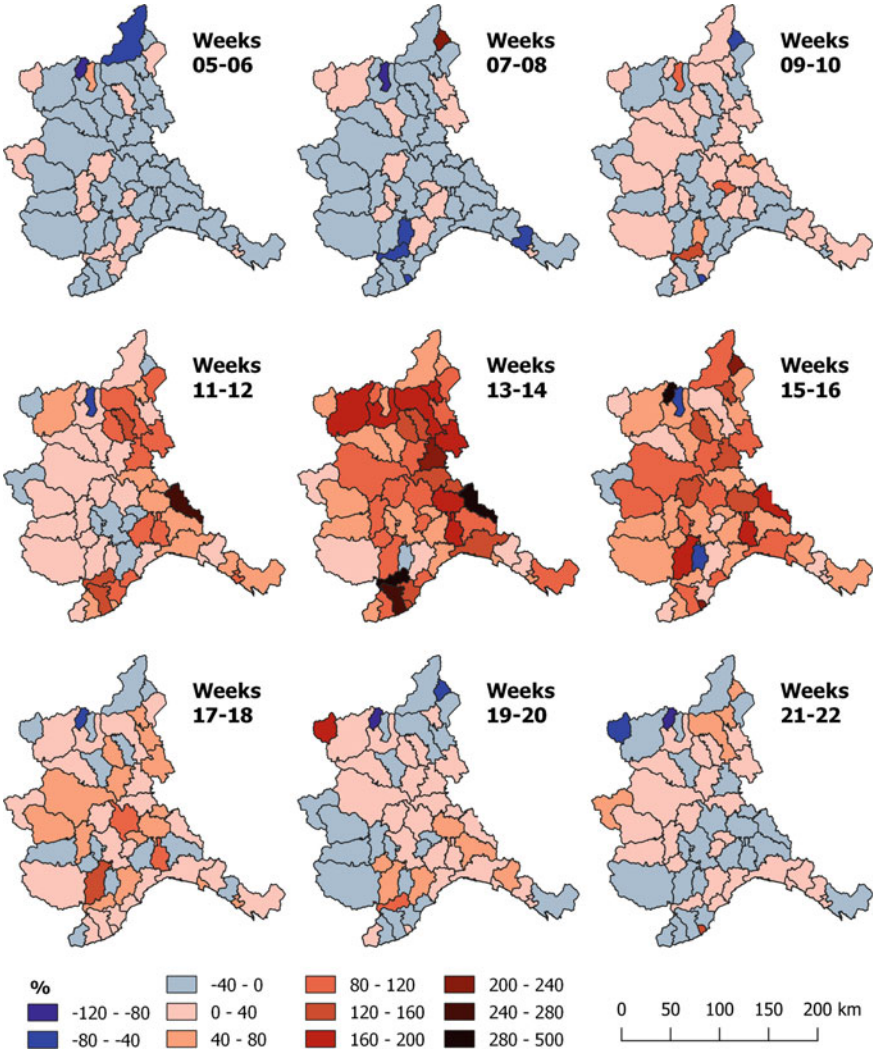


Fig. 7.5 Excess mortality for LLS

a *p*-value of 5.12e−05. Another pattern is shown in the cartogram of the proportion of the elderly population where the local systems of Liguria region are all part of the upper classes (Fig. 7.8b).

While, in the two cartograms of the self-containment of the job market indices (Fig. 7.8c, d) no scheme emerges but the local system of the regional capitals have the highest values in both indices, which is predictable as they are strong centers of attraction for labor.

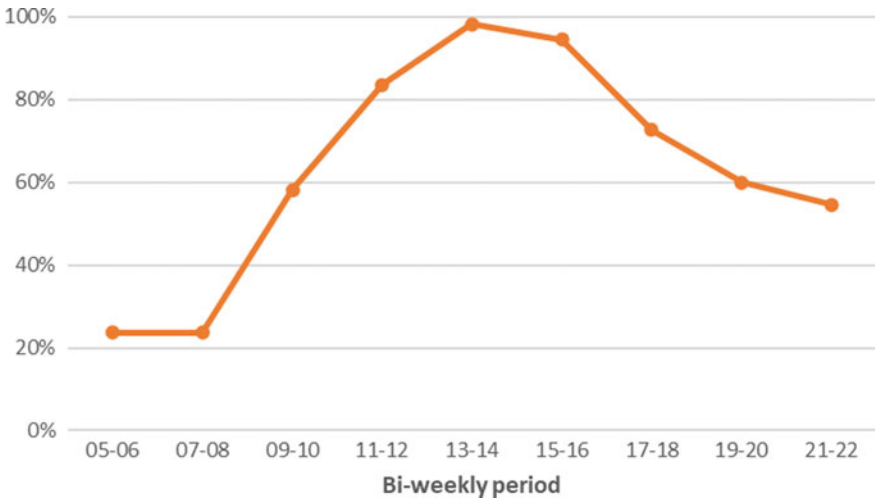


Fig. 7.6 Excess mortality trend

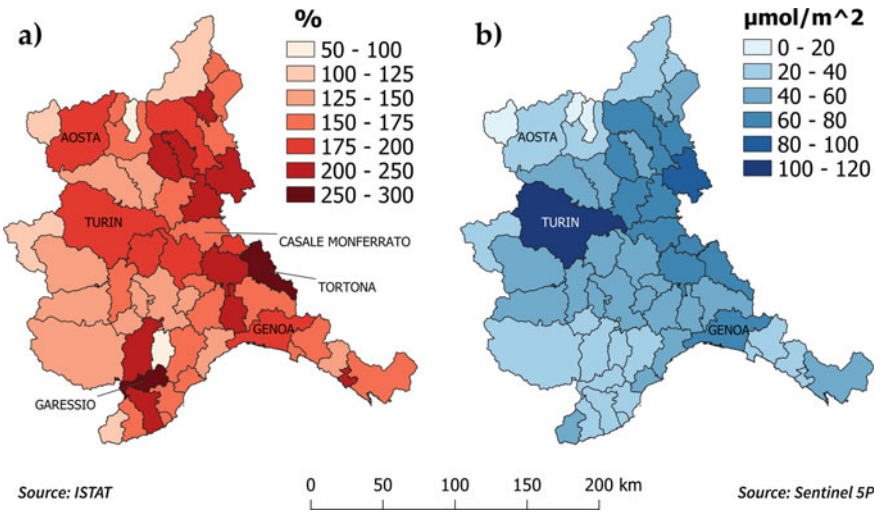


Fig. 7.7 **a** Excess mortality; **b** average concentrations of NO_2

7.3.2 Statistical Analysis

Spearman's correlation coefficient revealed that excess mortality during the first wave is moderately correlated to nitrogen dioxide concentrations ($\rho = 0.43$, p-value < 0.05), as evidenced by the regression line in the scatterplot in Fig. 7.9.

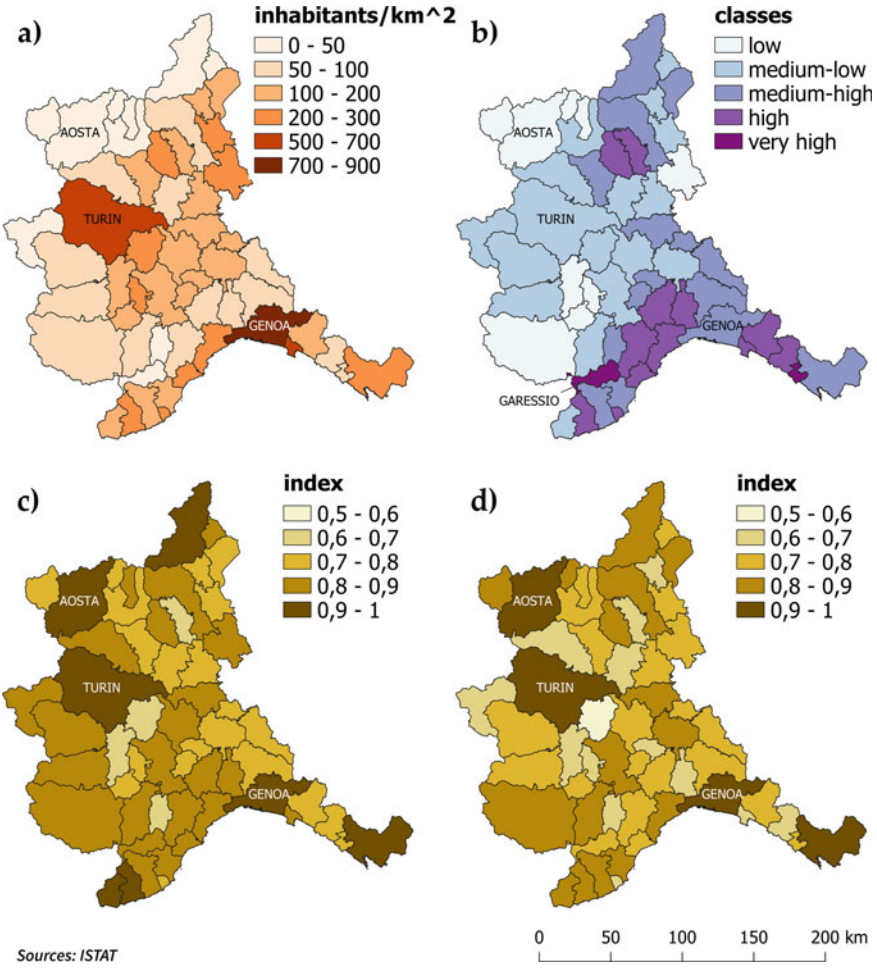


Fig. 7.8 **a** Population density (2020); **b** proportion of elderly population[3]; **c** self-containment index of the jobs demand (SCID); **d** self-containment index of the jobs supply (SCIS)

Subsequently, this correlation was also investigated using three quasi-Poisson regression models. Since the resulting coefficients of the regression models are reported on a logarithmic scale, they must be antilog to obtain rate ratios in the original scale for a better interpretation. Therefore, in the conversion process with the exponential function, some variables have been further transformed. The coefficients of NO_2 concentrations were multiplied for 10 so the rate ratio expresses the percent variation in excess mortality for each variation of 10 $\mu mol/m^2$. Similarly, other coefficients were transformed: the population density was multiplied for 100 so

[3] The classes were defined using the mean value and adding or subtracting one and two standard deviations.

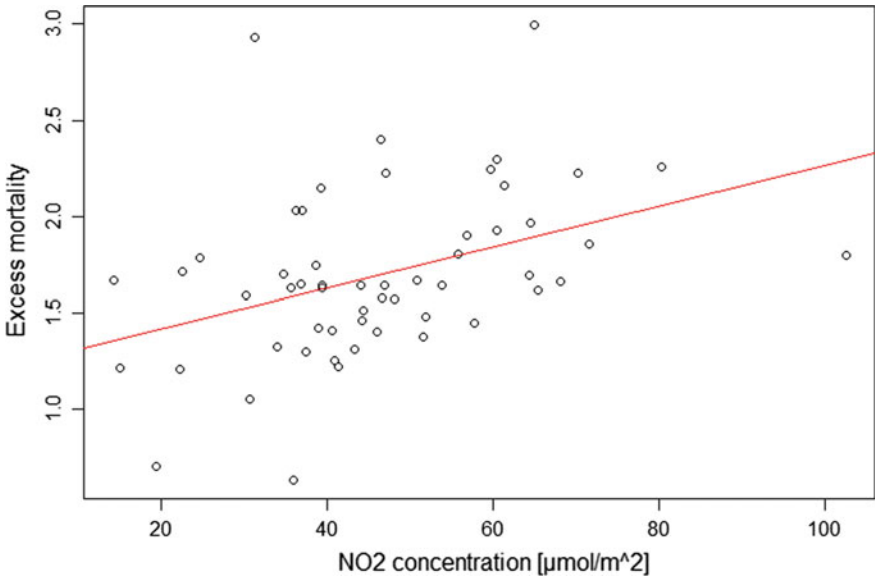


Fig. 7.9 Scatterplot: excess mortality versus NO_2 concentrations

Table 7.1 Values resulted from the regression in the first model (already retransformed)

Variables	Rate ratio	2.50%	97.50%	*p*-value
NO_2 concentration	1.01497	1.00332	1.02671	0.01450*

***$p < 0.001$; **$p < 0.01$; *$p < 0.05$

the rate ratio indicates the percent variation in excess mortality for a variation of 100 inhabitants/km^2. While, the coefficients of the two population proportions and the two self-containment indices (SCI) were divided by 100 so the rate ratios measures the percentage change in excess mortality for a one percentage point change in these indices.

In the first model, only the two main variables (NO_2 concentration and excess mortality) of the study were considered. As given in Table 7.1, each increase of 10 µmol/m^2 in NO_2 concentrations is associated with a 1.49%[4] (95%CI: 0.33 ÷ 2.67) increase in excess mortality.

Next to this, other variables were also considered for a possible confounding effect. These other two models differ for just one variable: one model considers the self-containment index of demand ("demand model") and the other the self-containment index of supply ("supply model"). In the "demand model" (Table 7.2), among all the variables, the only one statistically associated with the excess of mortality is the demand SCI variable.

[4] All the percentages are obtained subtracting 1 from the rate ratio values and multiplying it by 100.

Table 7.2 Values resulted from the regression in the "demand model" (already retransformed)

Variables	Rate ratio	2.50%	97.50%	*p*-value
NO_2 concentration	1.01813	0.99956	1.03714	0.06230
Population density	1.00314	0.98176	1.02489	0.77640
Over 65 population	1.02050	0.99696	1.04443	0.09380
Male population	0.98476	0.89891	1.07768	0.74150
Jobs per capita	2.46034	0.76704	7.94295	0.13770*
Demand SCI				

***$p < 0.001$; **$p < 0.01$; *$p < 0.05$

Table 7.3 Values resulted from the regression in the "supply model" (already retransformed)

Variables	Rate ratio	2.50%	97.50%	*p*-value
NO_2 concentration	1.01886	1.00081	1.03731	0.04643*
Population density	1.00352	0.98304	1.02434	0.73929
Over 65 population	1.02380	1.00064	1.04734	0.04886*
Male population	0.97373	0.88973	1.06459	0.56364
Jobs per capita	6.37255	1.61164	2.553444	0.01150*
Supply SCI	0.99352	0.98899	0.99806	0.00751**

***$p < 0.001$; **$p < 0.01$; * $p < 0.05$

Table 7.3 shows the rate ratios of the "supply model" in which four variables result associated with excess mortality. The associated percentage increase in excess mortality is 1.88% for each 10 μmol/m^2 increase in NO_2 concentration and 2.38% for one percentage point increase in the elderly population proportion. While, for an increase of one job per capita, the excess mortality is sixfold.

Both self-containment indices have an inverse association with the excess mortality indicated by the fact that both rate ratios are less than one. This inverse association means that each increase in one percentage point of the index is associated with a decrease in the excess mortality, respectively, of—0.65% for the demand SCI and—0.64% for the supply SCI.[5]

Moreover, in both two models, the variables of population density and the proportion of the male population do not find a significant association with excess mortality.

[5] In these cases subtracting one from the rate ratio resulted in the following calculations: "0.99341 − 1 = − 0.00659" for the SCID and "0.99352 − 1 = − 0.00648" for the SCIS.

7.4 Discussion and Conclusions

The relationship between NO_2 concentration and excess mortality investigated in this study partially emerges from the comparison of the respective cartograms. As previously described, these two variables tend to show higher values along the border with Lombardy region, particularly evident for the nitrogen dioxide pollutant. The zoning of NO_2 values follows the spatial distribution of the population density. This result is an expected consequence since more polluting sources (i.e., industries and vehicular traffic) tend to reside in the most populated areas.

The pattern of the highest excess mortality values near the Lombardy region needs more clarification: Lombardy region was the epicenter of the pandemic in Italy, and this explains how the local systems closest to the border have a higher excess of mortality, with a decreasing gradient toward West. However, this gradient is nonlinear as proximity is not the only contributing factor to the spread of the virus. In facts, an important element to consider is the degree of relations and connections that each local system has with other local systems. The more distant but more connected local systems, such as the Turin one, could be more affected by the spread of the virus than the systems closer to Lombardy but less connected, i.e., Casale Monferrato. For other local systems such as Garessio, the reason of high excess mortality value could be linked to the remarkably high value in the proportion of the elderly population. However, this kind of observations based on the comparison between only two variables could lead to misinterpretation of the real relationship; hence, statistical analyses are needed to consolidate preliminary observations. The nitrogen dioxide concentrations result associated to the excess mortality in two of the three regression models implemented. Our finding is therefore in accordance with previous studies (Filippini et al. 2021; Fattorini and Regoli 2020; Ogen 2020). In the "supply model", other variables, considered as confounders, showed a statistically significant association with the excess mortality. In the case of the proportion of the elderly population this result is congruent with the high incidence rate of COVID-19 in elderly people reported by the Italian National Institute of Statistic (ISTAT 2021b). Among the variables associated with excess mortality, the rate ratio with the greatest multiplicative effect is the one referred to the jobs per capita: since the period with higher excess mortality values coincides with the national lockdown, when the only movements allowed were mainly for work reasons. The number of jobs in a local system was critical for the spread of the virus because it increased the intensity of travels and the amount of close contacts between coworkers. Therefore, it can be assumed as the cause of such a great multiplicative effect. An unexpected result is the non-association of population density with excess mortality; in fact, a greater population density should correspond to a greater possibility of interpersonal contacts and therefore more infections. An interesting interpretation of this is provided by the study of Cremaschi et al. (2021) which suggests the adoption of a *relational density* (McFarlane 2016) to justify the spatial spread of the virus. Density can be considered a measure of how close social relations are in the resident population. The use of this variable would allow to highlight substantial differences in socio-spatial relationship

that characterize small- or medium-sized territorial systems compared to those of large cities.

The two self-containment indices were used as a measure of the isolation of the local systems. Higher values correspond a smaller number of workers who arrive from outside the system or who leave the system in which they live to work outside. The inverse association with the excess mortality demonstrated by both indices means that a system with a higher SCI, net of other variables, recorded a lower excess mortality during the first wave of the pandemic. This relationship could be explained as lower exchanges of workers with other local systems. In an initial phase of the spread of the virus, when it was not yet homogeneously present on the territory, exchanges with external systems were essential for its transmission. Furthermore, considering that the only travels allowed during the lockdown period were those related to work, this fact strengthen the role of these indices in the interpretation of the spread of the disease.

The multivariate regression models carried out confirmed the existence of a significant statistical association between NO_2 concentrations and excess mortality values for local systems of the northwestern regions during the first COVID-19 epidemic wave in Italy.

The results obtained are thus part of a broader panorama of studies aimed at evaluating the effects of air pollution on human health (Carugno et al. 2016; Eum et al. 2019; Fattorini and Regoli 2020; Filippini et al. 2020; Ogen 2020) but also highlight the importance of conducting such analyses on a more appropriate geographic scale such as that of local systems.

Acknowledgements Here we want to thank Giovenale Moirano (MD-Ph.D., University of Turin) for the precious scientific contribution he has provided us.

References

Berk R, MacDonald JM (2008) Overdispersion and Poisson regression. J Quant Criminol 24:269–284. https://doi.org/10.1007/s10940-008-9048-4

Carugno M, Consonni D, Randi G, Catelan D et al (2016) Air pollution exposure, cause-specific deaths and hospitalizations in a highly polluted Italian region. Environ Res 147:415–424. https://doi.org/10.1016/j.envres.2016.03.003

CIESIN (2018). Gridded population of the world, Version 4 (GPWv4): population count, Revision 11. NASA Socioeconomic Data and Applications Center (SEDAC). https://sedac.ciesin.columbia.edu/data/set/gpw-v4-population-count-rev11

Ciminelli G, Garcia-Mandicó S (2020) COVID-19 in Italy: an analysis of death registry data. J Public Health 42(4):723–730. https://doi.org/10.1093/pubmed/fdaa165

Coccia M (2020) Factors determining the diffusion of COVID-19 and suggested strategy to prevent future accelerated viral infectivity similar to COVID. Sci Total Environ 729:138474. https://doi.org/10.1016/j.scitotenv.2020.138474

Conticini E, Frediani B, Caro D (2020) Can atmospheric pollution be considered a cofactor in extremely high level of SARS-CoV-2 lethality in Northern Italy? Environ Pollut 261:114465. https://doi.org/10.1016/j.envpol.2020.114465

Cremaschi M, Salone C, Besana A (2021) Densità urbana e Covid-19: la diffusione territoriale del virus nell'area di Bergamo. Archivio Di Studi Urbani e Regionali 131:5–31. https://doi.org/10.3280/ASUR2021-131001

DPCM (2020a) Decreto del Presidente del Consiglio dei Ministri 9 marzo 2020. Tratto da Gazzetta Ufficiale della Repubblica Italiana. https://www.gazzettaufficiale.it/eli/id/2020/03/09/20A01558/sg

DPCM (2020b) Decreto del Presidente del Consiglio dei Ministri 26 aprile 2020. Tratto da Gazzetta Ufficiale della Repubblica Italiana. https://www.gazzettaufficiale.it/eli/id/2020/04/27/20A02352/sg

Eum K-D, Kazemiparkouhi F, Wang B, Manjourides J, Pun V, Pavlu V, Suh H (2019) Long-term NO_2 exposures and cause-specific mortality in American older adults. Environ Int 124:10–15. https://doi.org/10.1016/j.envint.2018.12.060

Fattorini D, Regoli F (2020) Role of the chronic air pollution levels in the Covid-19 outbreak risk in Italy. Environ Pollut 264:114732. https://doi.org/10.1016/j.envpol.2020.114732

Filippini T, Rothman KJ, Vinceti M (2021) Associations between mortality from COVID-19 in two Italian regions and outdoor air pollution as assessed through tropospheric nitrogen dioxide. Sci Total Environ 760:143355. https://doi.org/10.1016/j.scitotenv.2020.143355

Filippini T, Rothman KJ, Goffi A, Ferrari F, Maffeis G, Orsini N, Vinceti M (2020). Satellite-detected tropospheric nitrogen dioxide and spread of SARS-CoV-2 infection in Northern Italy. Sci Total Environ 739. https://doi.org/10.1016/j.scitotenv.2020.140278

ISTAT (2015a) Sistemi locali del lavoro - Nota metodologica. Report statistiche. Roma, Istat. https://www.istat.it/it/files//2014/12/nota-metodolgica_SLL2011_rev2015a0205.pdf

ISTAT (2015b) Indicatori di qualità dei sistemi locali del lavoro. Roma. Istat. https://www4.istat.it/it/strumenti/territorio-e-cartografia/sistemi-locali-del-lavoro/indicatori-di-qualit%C3%A0-sll

ISTAT (2020a) Composizione dei Sistemi Locali del Lavoro 2011 a patire dal 1° gennaio 2020. Roma, Istat. https://www.istat.it/it/archivio/252261

ISTAT (2020b) I.stat, Popolazione residente al 1° gennaio. Roma. Istat. http://dati.istat.it/Index.aspx?QueryId=19101

ISTAT (2021a) Dataset con i decessi giornalieri. Roma, Istat. https://www.istat.it/it/archivio/240401

ISTAT (2021b) Impatto dell'epidemia covid-19 sulla mortalità totale della popolazione residente. V Rapporto, 5 marzo 2021. https://www.istat.it/it/files//2021/03/Report_ISS_Istat_2020_5_marzo.pdf

Martelletti L, Martelletti P (2020) Air pollution and the novel Covid-19 disease: a putative disease risk factor. SN Compr Clin Med 2(4):383–387. https://doi.org/10.1007/s42399-020-00274-4

McFarlane C (2016) The geographies of urban density: topology, politics and the city. Prog Hum Geogr 40(5):629–648. https://doi.org/10.1177/0309132515608694

Ogen Y (2020) Assessing nitrogen dioxide (NO_2) levels as a contributing factor to coronavirus (COVID-19) fatality. Sci Total Environ 726:138605. https://doi.org/10.1016/j.scitotenv.2020.138605

Pignocchino G, Pezzoli A, Besana A (2022) Satellite data and epidemic cartography: a study of the relationship between the concentration of NO_2 and the COVID-19 epidemic. In: Borgogno-Mondino E, Zamperlin P (eds) Italian conference on geomatics and geospatial technologies. Springer International Publishing, Cham, pp 55–67

Open Access This chapter is licensed under the terms of the Creative Commons Attribution 4.0 International License (http://creativecommons.org/licenses/by/4.0/), which permits use, sharing, adaptation, distribution and reproduction in any medium or format, as long as you give appropriate credit to the original author(s) and the source, provide a link to the Creative Commons license and indicate if changes were made.

The images or other third party material in this chapter are included in the chapter's Creative Commons license, unless indicated otherwise in a credit line to the material. If material is not included in the chapter's Creative Commons license and your intended use is not permitted by statutory regulation or exceeds the permitted use, you will need to obtain permission directly from the copyright holder.

